

Specific Heat and Scaling of ^4He Confined in a Planar Geometry

Sarabjit Mehta and Francis M. Gasparini

State University of New York at Buffalo, Buffalo, New York 14260

(Received 8 November 1996)

We report measurements of the specific heat of thick helium films to test scaling predictions near the superfluid transition, T_λ . These films, bounded by two silicon wafers, range in thickness from 0.107 to 0.692 μm . The specific heat of the films is suppressed relative to that of bulk helium, and the difference of the data from bulk helium scales well with the exponent of the correlation length. We propose an empirical scaling function which fits the data well for $T > T_\lambda$, and yields the surface specific heat. We also compare the data with various theoretical calculations and experiments. We find that the calculations underestimate the effect of confinement. [S0031-9007(97)02843-3]

PACS numbers: 67.40.Kh, 65.20.+w, 67.70.+n

The motivation for this work was to study effects of confinement on the heat capacity of liquid ^4He near the superfluid transition temperature, T_λ . Compared to bulk helium, the heat capacity of a finite sample is suppressed, and the maximum is rounded and shifted below T_λ . The magnitude of these effects depends on the confinement size L , boundary conditions, and, if appropriate, the lower crossover dimension of the confined system.

According to correlation length scaling [1] it is expected that these effects depend on the variable ξ/L , where $\xi = \xi_0|t|^{-\nu}$ is the divergent bulk correlation length, with $\nu = 0.6705$ [2], and $t = T/T_\lambda - 1$. This scaling has come into question from a number of experiments [3,4], while others, done for a single confinement [5,6], have found consistency with this prediction. We report here the first measurements of heat capacity for a series of equivalent planar confinements which support scaling.

The scaling functions $f_1(tL^{1/\nu})$ and $f_2(tL^{1/\nu})$ for the heat capacity have been calculated using field theory [7],

$$[C(t, \infty) - C(t, L)]t^\alpha = (tL^{1/\nu})^\alpha f_2(tL^{1/\nu}), \quad (1)$$

$$[C(t, L) - C(t_0, \infty)]L^{-\alpha/\nu} = f_1(tL^{1/\nu}), \quad (2)$$

where t_0 is defined by $\xi(t_0) = L$. α is the exponent of the heat capacity [8]. The function $f_1(tL^{1/\nu})$, valid throughout the transition region, has also been determined via Monte Carlo simulations of the XY model [9].

In order to test these predictions, one needs a range of uniform confinement sizes. In our experiments, this is achieved by confining helium films between two, 2 in diameter silicon wafers. One wafer has a SiO_2 pattern made lithographically consisting of a triangular array of squares ($0.25 \times 0.25 \text{ mm}^2$, 1 mm apart) [4], surrounded by a 4 mm wide circular border. The thickness of the SiO_2 defines the confinement size. The other wafer has a small central hole used to introduce helium into the cell. These two wafers are bonded together using direct wafer bonding [10,11]. This improves our earlier protocol [12], and is much more reliable. Diagnostics of the

bonding quality include infrared (IR) imaging and IR interference experiments [11,12]. From the latter, the separation between the bonded wafers can be measured at various positions. This is shown in Fig. 1 as a continuous surface. The gap between the wafers has about 1% uniformity. Its magnitude is in good agreement with the SiO_2 thickness determined by ellipsometry after the oxide growth process. After bonding, the wafers are assembled for ac calorimetry [13]. A film heater is evaporated on the wafers; they are connected to a stainless steel fill line and mounted on the cryostat, Fig. 2. The central structure involving the nickel sleeve is designed to interface the silicon with the metal structure of the filling line and avoid difficulties associated with differential contraction [12]. Germanium thermometers, θ_1 and θ_2 , are used to regulate the cell temperature and measure the heat capacity signal. The regulation is done with a time constant much longer than the period of ac oscillations and has no effect on the heat capacity signal. Two isothermal stages are used to prevent temperature inversion in the cell by keeping $T_{S1} > T_{\text{cell}} > T_{S2}$. The heat drain on top of the cell is via a webbing of indium wires connected to a copper wire leading to S_2 .

The heat capacity is measured using a heating frequency varying from 10 to 40 Hz for different cells. The response of each cell, with and without helium, is studied throughout the transition region to determine the operating frequency, and the relation of the signal amplitude to the heat capacity. This frequency is then kept constant for a given cell. The temperature oscillations, which are at the simplest inversely proportional to the heat capacity, are picked up as voltage signals. These signals are averaged from 1 to 5 min. This allows one to make high precision measurements on μ -mole size samples using temperature oscillations of only a few μK in amplitude. When the cell is filled, helium is allowed to fill a small portion of the center Si piece, Fig. 2. Thus, if the cell temperature is allowed to drift slowly, the drift rate is sensitive to the heat capacity of the bulk helium present in the fill line region. This causes a kink in the rate of temperature change at T_λ , and yields T_λ to within $\pm 1.5 \mu\text{K}$. The bulk helium also

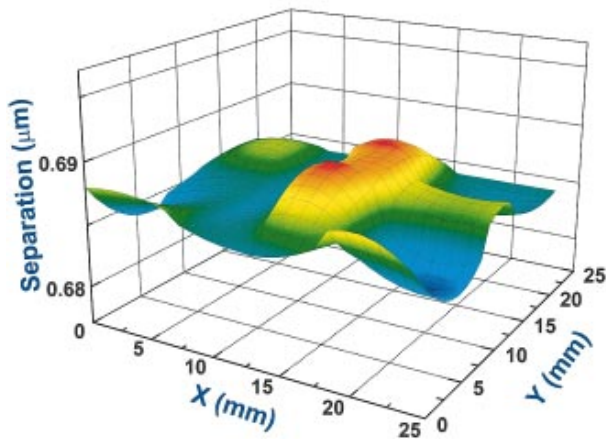


FIG. 1(color). Measured separation between two bonded wafers. The surface in this figure is constructed from 30 individual measurements on a $25 \times 25 \text{ mm}^2$ grid on the surface of the wafers.

has a relatively large thermal mass which enhances the long term temperature stability but prevents it from contributing to the ac oscillations. This was verified explicitly by measuring a single wafer with and without helium in the filling line. The heat capacity of the wafer plus addenda actually *decreases* a small amount when helium is present in the fill line because of the thermal loading of the center structure. We allow for this in our data analysis. The background heat capacity, measured for each cell, is in the range of $30\text{--}40 \mu\text{J/K}$ near T_λ .

The specific heat of helium as a function of reduced temperature for various confinements is shown in Fig. 3. In this plot the heat capacity breaks up into two branches,

one above and one below T_λ . The bulk specific heat [14] appears as two nearly parallel lines. The heat capacity of the confined helium is suppressed and is *continuous through* T_λ . For $T > T_\lambda$, the data for the larger films asymptote to within 1% of the expected value based on the geometry of the cell. For $T < T_\lambda$, the heat capacity maximum is rounded and shifted further below T_λ the smaller the confinement. However, for this branch we measure asymptotically in some cases an excess of heat capacity, and also observe a shoulder below the heat capacity maximum. *These features manifest after the helium in the cell becomes superfluid, i.e., below the maximum.* They are due to two mechanisms: the coupling via the superfluid in the cell to the center region *under* the silicon piece, and the onset of a resonance mode which we have called adiabatic fountain resonance [15]. This can be used to determine the superfluid fraction, but, at the same time, interferes with the heat capacity signal by distorting the frequency response. Thus, data for $T < T_\lambda$ have to be truncated for the scaling analysis slightly *below* the heat capacity maximum.

Scaling plots for the data are shown in Fig. 4 for both above and below T_λ . We find that $\nu = 0.6705$ [2] gives good collapse of the data onto universal curves [16]. The collapse is best for $T > T_\lambda$, and there are, perhaps, some small systematic differences for $T < T_\lambda$ near the maximum. It is possible that these might be due to nonuniversal aspects associated with 2D crossover. For $T > T_\lambda$, where the collapse is over nearly 5 decades in the scaling variable, $x = tL^{1/\nu}$, we find *qualitative* agreement with theoretical calculation of f_2 [7]. The theory, however, *underestimates* the effect of confinement

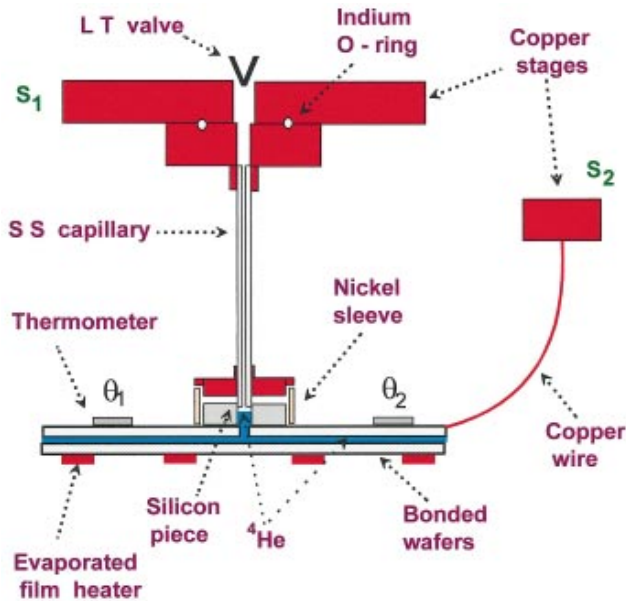


FIG. 2(color). Arrangement of experimental cell for ac calorimetry. Drawing is schematic and not to scale.

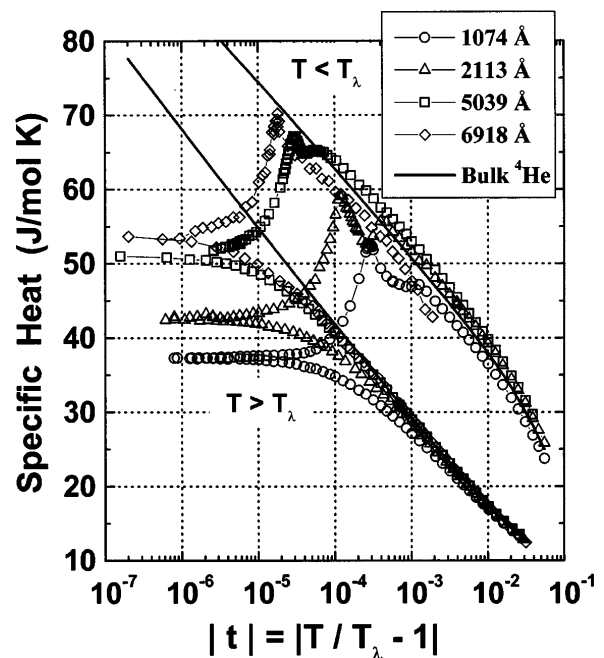


FIG. 3. Specific heat for four planar confinements.

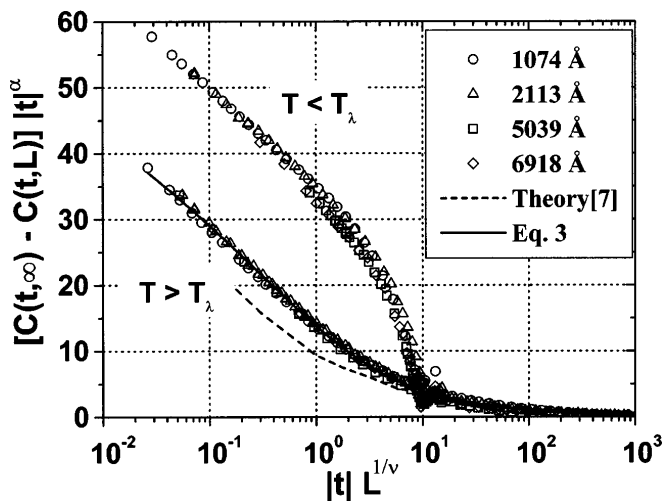


FIG. 4. Scaling of the specific heat for various confinement sizes, $\nu = 0.6705$, L is in \AA , the specific heat in J/mol K.

for small x . The data are suppressed more and so lie above the theory in this plot. The range of data for the $T < T_\lambda$ branch have to be limited to slightly below the maximum for the reasons discussed above. We believe the collapse shown in Fig. 4 is the first for a series of heat capacity measurements for planar confinement on any system.

We also compare the data with Monte Carlo simulations [9] and the function f_1 [7] in Fig. 5. The data again show good collapse but do not agree quantitatively with the calculation. As before, the calculations underestimate the effect of confinement, particularly in the re-

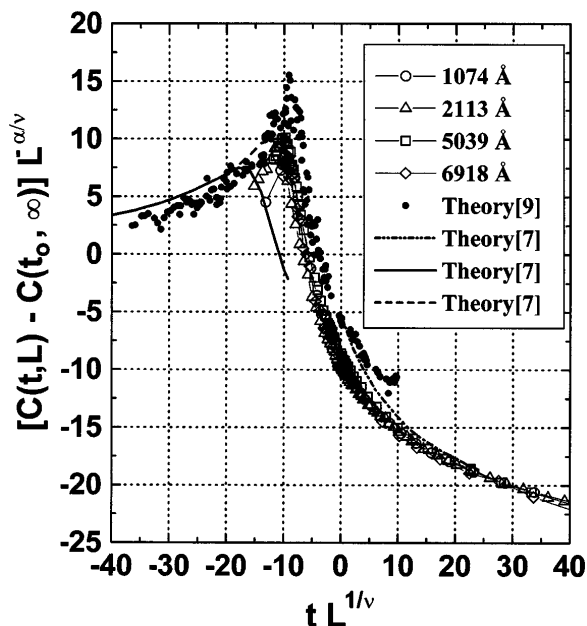


FIG. 5. Comparison of specific heat data with theoretical calculations of the scaling function f_1 . L is in \AA , the specific heat in J/mol K.

gion $-10 < x < 10$. On this plot, this corresponds to the data falling below the theory.

We propose the following empirical scaling function for $T > T_\lambda$,

$$[C(t, \infty) - C(t, L)]t^\alpha = \frac{A/\alpha}{1 + ay^\nu} + \frac{by^\alpha}{1 + cy^{\alpha+\nu}}, \quad (3)$$

where we introduce a dimensionless variable $y = t(L/a_0)^{1/\nu} = x(a_0)^{-1/\nu}$, and the thickness of one atomic layer $a_0 = 3.56 \text{\AA}$. Also, $A/\alpha = -337 \text{ J/mol K}$ is the ratio of leading amplitude and exponent of $C(t, \infty)$; see Gasparini and Gaeta [14]. Equation (3) has the correct limit expected on a basis of a bulk-plus-surface division of the free energy [4,17], i.e., the surface specific heat. Also, as y becomes small, it has the correct dependence expected on the basis that $C(t, L)$ becomes a constant. The solid line through the data in Fig. 4 is a least squares fit to this function. The resulting parameters are $a = 1.747 \pm 0.073$, $b = 353.7 \pm 0.2 \text{ J/mol K}$, and $c = 1.765 \pm 0.071$. The surface specific heat, C_s , follows from Eq. (3) in the limit that $y \rightarrow \infty$,

$$\begin{aligned} \lim_{y \rightarrow \infty} [C(t, \infty) - C(t, L)]t^\alpha &= \left(\frac{A/\alpha}{a} + \frac{b}{c} \right) y^{-\nu} \\ &= \left(\frac{A/\alpha}{a} + \frac{b}{c} \right) \frac{a_0}{L} t^{-\nu}, \quad (4) \end{aligned}$$

$$[C(t, \infty) - C(t, L)] \frac{L}{2a_0} = -C_s, \quad (5)$$

$$C_s = -3.7 t^{-(\alpha+\nu)} \text{ J/mol K}, \quad (6)$$

where Eq. (5) is from Eq. (2.23) of Ref. [4], and Eq. (6) is obtained by using the given A/α and values of a , b , and c determined from the fit. From the large x limit of f_2 in Ref. [7] we estimate the amplitude for Eq. (6) to be -3.9 J/mol K . This is good agreement, which is expected since theory and data agree for large values of the scaling variable x ; see Figs. 4 and 5.

Last we compare our results with the data obtained for a series of cylindrical confinement in Nuclepore filters [3]. These represent crossover to 1D as ξ becomes large. These data yielded results which disagree with scaling. This conclusion was based on *an analysis which demanded scaling of these data together with data for unsaturated films of helium*. Further, the Nuclepore data yielded a scaling exponent much less than ν when fitted to a pure power law for the scaling function [17]. If one does not impose these constraints, and one ignores the data for 300\AA confinement, which are, in fact, the least precise, then the Nuclepore results are not inconsistent with the present results. The most significant difference between the Nuclepore and the present data is for $T < T_\lambda$ in the region of the minimum in the scaling function, Fig. 4, i.e., the *maximum* in the specific heat. In the case of the 1D crossover (cylindrical) the maximum has a smaller value than in the case of the 2D crossover (planar). This

translates into an inflection point in the scaling function rather than the deep minimum see in Fig. 4. This we believe is a significant difference in the data, and we associate it with the different crossover dimensionality.

This work was supported by the NSF, DMR9214010 and DMR9623831, and by the Cornell Nanofabrication Facility, 526-94. We are grateful to C. Schmitt for some of the optical measurements and to X. Wang for his contribution in the early phase of this work.

-
- [1] M.E. Fisher, in *Critical Phenomenon*, Proceedings of the International School of Physics "Enrico Fermi," Course LI, edited by M.S. Green (Academic Press, New York, 1971). See also M.N. Barber, in *Phase Transitions and Critical Phenomena*, edited by C. Domb and J.L. Lebowitz (Academic Press, New York, 1983), Vol. 8; V. Privman, in *Finite Size Scaling and Numerical Simulations of Statistical Systems*, edited by V. Privman (World Scientific, New Jersey, 1990).
- [2] L.S. Goldner and G. Ahlers, *Phys. Rev. B* **45**, 13 129 (1992).
- [3] T.-P. Chen and F.M. Gasparini, *Phys. Rev. Lett.* **40**, 331 (1978).
- [4] I. Rhee, F.M. Gasparini, and D.J. Bishop, *Phys. Rev. Lett.* **63**, 410 (1989). See also, F.M. Gasparini and I. Rhee, in *Progress in Low Temperature Physics*, edited by D.F. Brewer (North-Holland, New York, 1992), Vol. XIII.
- [5] J.A. Nissen, T.C.P. Chui, and J. Lipa, *J. Low Temp. Phys.* **92**, 352 (1993).
- [6] M. Coleman and J. Lipa, *Phys. Rev. Lett.* **74**, 286 (1995).
- [7] R. Schmolke, A. Wacker, V. Dohm, and D. Frank, *Physics B* **165–166**, 575 (1990). See also V. Dohm, *Phys. Scr.* **T49**, 46–58 (1993).
- [8] Using $\nu = 0.6705$ from Ref. [2], one obtains $\alpha = -0.0115$ using the relation, $\alpha = 2 - 3\nu$.
- [9] N. Schultka and E. Manousakis, *Phys. Rev. Lett.* **75**, 2710 (1995).
- [10] R. Stengl, K.-Y. Ahn, and U. Gosele, *Jpn. J. Appl. Phys.* **27**, L2364 (1988).
- [11] S. Mehta, W. Y. Yu, A. Petrou, J. Lipa, D. Bishop, and F.M. Gasparini, *Czech. J. Phys.* **46**, 133 (1996).
- [12] I. Rhee, D.J. Bishop, A. Petrou, and F.M. Gasparini, *Rev. Sci. Instrum.* **61**, 1528 (1990).
- [13] P.F. Sullivan and G. Seidel, *Phys. Rev.* **173**, 679 (1968).
- [14] F.M. Gasparini and M. Moldover, *Phys. Rev. B* **12**, 93 (1975); F.M. Gasparini and A.A. Gaeta, *Phys. Rev. B* **17**, 1466 (1978); F.M. Gasparini, Ph.D. thesis, University of Minnesota, 1970, available from University Microfilms International. These data have a wider range about T_λ than other data of comparable precision, and allow us to test the asymptotic approach of the present data to their bulk value.
- [15] F.M. Gasparini, S. Mehta, and X. Wang, *Czech. J. Phys.* **46**, 81 (1996).
- [16] S. Mehta and F.M. Gasparini, *Czech. J. Phys.* **46**, 173 (1996). In this preliminary report based on two confinement sizes, we concluded that the data do not support scaling. This was based on an incorrect analysis of the 5039 Å data.
- [17] F.M. Gasparini, T.P. Chen, and B. Bhattacharyya, *Phys. Rev. B* **23**, 5797 (1981).